FORMATION OF THE SUPERCLUSTER-VOID NETWORK

J. EINASTO
Tartu Astrophysical Observatory, EE-2444, Estonia

1. Evidence

Already first redshift surveys, made 10 – 15 years ago, demonstrated that galaxies and clusters of galaxies are located along patchy sheets and filaments, and the space between is empty. Sheets and filaments form large aggregates – superclusters of galaxies. Between superclusters there are large voids with no clusters at all, in such supervoids we observe only poor galaxy filaments (Lindner *et al.* 1994).

Deep pencil-beam survey in the direction of the North and South galactic poles has found that high-density peaks in the distribution of galaxies are spaced in a surprisingly regular pattern with distance of about 128 h^{-1} Mpc between them (Broadhurst *et al.* 1990). More recently, an ESO Key Project to survey faint galaxies in a two-dimensional sheet suggests the presence of circular high-density regions which surround low-density areas. The mean diameter of these structures is also about 128 h^{-1} Mpc (Vettolani *et al.* 1994). The power spectra of the density distributions in these one- and two-dimensional surveys have maxima at about 128 h^{-1} Mpc (Broadhurst *et al.* 1990, Vettolani *et al.* 1994).

These one- and two-dimensional surveys have been complemented by three-dimensional surveys of clusters of galaxies. These studies have shown that superclusters and supervoids form a fairly regular network of high- and low-density regions, traced by rich clusters of galaxies (Bahcall 1991, Tully *et al.* 1992, Einasto *et al.* 1994b). This is illustrated in Figure 1, which shows the distribution of rich clusters in a 600 h^{-1} Mpc rectangle in supergalactic coordinates (h is the Hubble constant in units of 100 km/s/Mpc). The mean separation between high-density peaks in this distribution is approximately 130 h^{-1} Mpc. High-density peaks are located in a fairly rectangular grid which forms a three-dimensional chessboard (Tully *et al.* 1992).

M. Kafatos and Y. Kondo (eds.), Examining the Big Bang and Diffuse Background Radiations, 193–200.

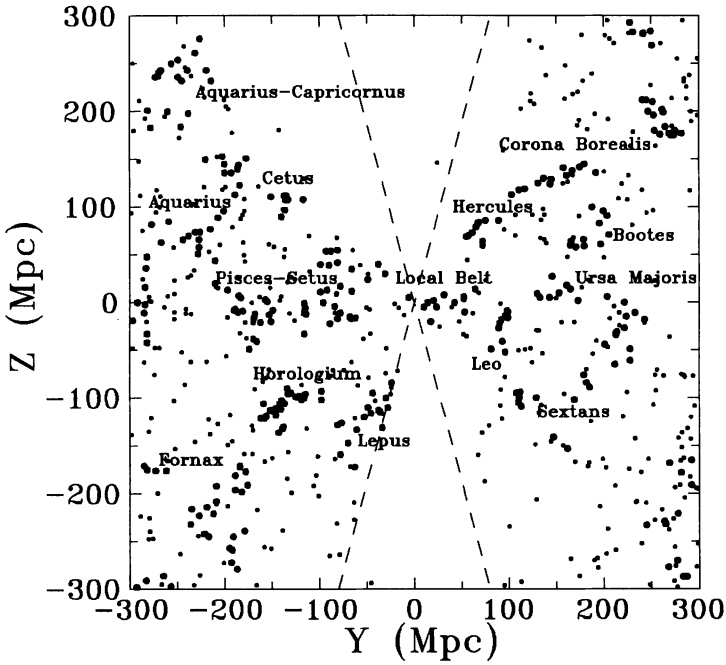

Figure 1. The distribution of clusters of galaxies in supergalactic coordinates, the sheet is taken in between supergalactic $-100 \leq X < 100\ h^{-1}$ Mpc. Clusters belonging to rich superclusters (containing at least 4 clusters) are plotted with filled circles, clusters located in poor superclusters as small dots. Superclusters are identified by common names (from constellations where they are located). Dashed lines mark the zone of avoidance near the galactic plane.

The presence of a 130 h^{-1} Mpc scale in the distribution of rich clusters of galaxies has been demomstrated also by Mo *et al.* (1992a, b) by the study of the correlation function on large separations.

Below we concentrate to the explanation of this semiregular supercluster-void structure. We report on simulations of the formation of the large-scale structure using CDM-type models and models with simple double power spectra. We compare the distribution of simulated galaxies and clusters of galaxies in models with the observations. We compare also the power spectra and the cluster correlation functions of simulations with observations. Our principal conclusion is that CDM-type models, both high- and low-density, are incompatible with available observational data.

2. Models

The observed structure is formed from initially small density perturbations. The amplitude of density perturbations on different scales is characterized by the power spectrum of the density field. The power spectrum can be

https://doi.org/10.1017/S0074180900110071 Published online by Cambridge University Press

approximated by a double power law with one power index n_l on large scales, another index n_s on small scales, and with the transition between power indices at a wavelength λ_t,

$$P(k) = \begin{cases} A\kappa^{n_s}, & \text{if } k \geq k_t \\ A\kappa^{n_l}, & \text{if } k < k_t. \end{cases}$$

Here A is the amplitude, $\kappa = k/k_t$, and the wavenumber k is related to the wavelength as follows: $\lambda = 2\pi/k$.

We also used initial spectra from theoretical models, such as the Cold Dark Matter (CDM) scenario of structure formation,

$$P(k) = A \frac{k}{\left(1 + \frac{(ak)^2}{\log(1+bk)}\right)^2}.$$

In this formula the parameters are as follows: $a = 4.0/(\Omega h^2)$, $b = 2.4/(\Omega h^2)$, h is the Hubble constant, and Ω is the density parameter in units of the critical closure density. The values of constants a and b correspond to wavelength λ, expressed in h^{-1} Mpc.

CDM-type spectra in combination with power-law spectra enable us to investigate the impact of the character of the transition between large and small wavelengths. The essential difference between those models is the scale length over which this transition occurs. In the power-law models the transition is sudden, and is much more smooth in the CDM models.

We performed numerical simulations of the formation and evolution of the large-scale structure of the universe by changing initial parameters of the models. A detailed description of all models shall be published elsewhere (Saar *et al.* 1994, Frisch *et al.* 1994). Parameters of principal models are given in Table 1. Models were calculated using a PM code using 128^3 particles and cells. In the table we give the size of the computational box L, the density parameter Ω (for the low-density CDM model we assume the presence of a cosmological term Ω_Λ, where $\Omega + \Omega_\Lambda = 1$), and the rms amplitude of density perturbations on 8 h^{-1} Mpc scale σ_8. In CDM-models we have adopted the Hubble constant $h = 0.5$. Models which are not shown in Table 1 include power-law spectra with different values of power indexes n_l and n_s, and models using a single power-law as the initial spectrum.

The evolution of the distribution of particles in the N-body code represents the evolution of the dark matter distribution. Clustered particles, i.e. particles associated with galaxies and their dark haloes, were selected according to the density smoothed in 1 h^{-1} Mpc scale: all particles located at density higher than the mean density were considered as clustered. Clusters of galaxies were identified as high-density peaks in the distribution of dark matter smoothed with a Gaussian window with a dispersion of 1 h^{-1} Mpc.

TABLE 1. Data on models

Model	Ω	h	n_l	n_s	λ_t h^{-1} Mpc	L h^{-1} Mpc	σ_8
N2p	1	0.5	1	−1.5	128	512	0.90
CDM1	1	0.5	1	−0.5	64:	512	0.70
CDM2	0.2	0.5	1	−1.5	500:	512	0.85

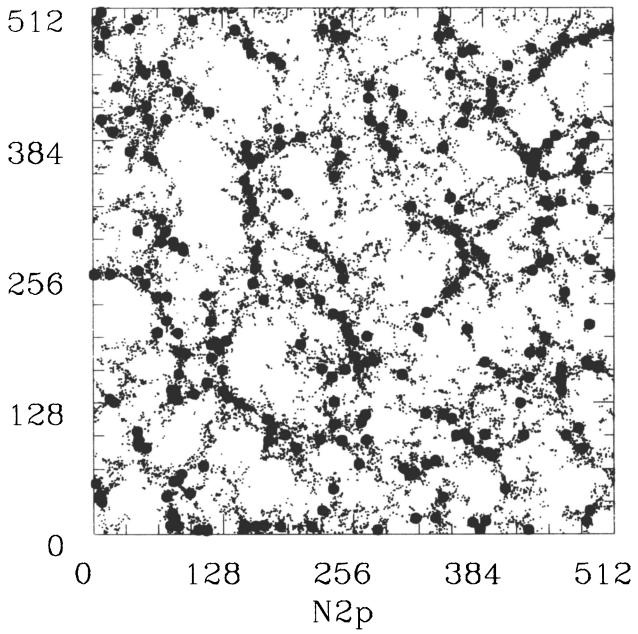

Figure 2. The distribution of simulated galaxies (dots) and clusters of galaxies (filled circles) in the double power law simulation N2p. Note the concentration of galaxies and clusters to ring-like structures separated by about 128 h^{-1} Mpc.

The number density of clusters has been taken equal to the number density of Abell clusters. Superclusters of galaxies were identified as high-density regions smoothed with 8 h^{-1} Mpc smoothing length.

3. Cosmography of galaxies and clusters

An example of the final structure in a model with a sharp transition in the power spectrum is shown in Figure 2. Both, the distribution of simulated galaxies and clusters of our model N2p are plotted.

Figure 2 shows that the distribution of galaxies is well ordered. Rich

https://doi.org/10.1017/S0074180900110071 Published online by Cambridge University Press

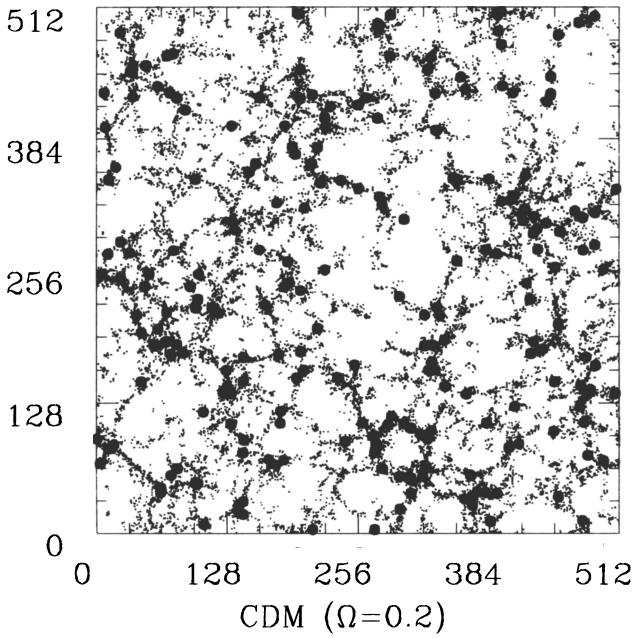

Figure 3. The distribution of simulated galaxies and clusters in the low-density model CDM2. The location of high-density regions is much less regular than in the model N2p.

clusters of galaxies are located in high-density regions (superclusters) which surround regions of low density (supervoids). High-density regions have circular shapes. The mean distance of high-density regions across supervoids is equal to the scale of the maximum, λ_t. Simulated galaxies form filaments both in superclusters and in supervoids as in the real Universe (Lindner *et al.* 1994). The density of filaments is different: in superclusters they consist of chains of rich clusters, in supervoids of chains of galaxies.

For comparison we show in Figure 3 the distribution of simulated galaxies and clusters of galaxies in a low-density model CDM2. In this model, the power spectrum of density fluctuations has a maximum just at the wavelength equal to the size of the simulation box. Due to the flat maximum high-density regions (superclusters and rich clusters of galaxies) are much less organized than in the previous model. Diameters of voids between superclusters have a large scatter.

Our conclusion from these simulations and a number of others not shown here is that a semiregular pattern of high- and low-density regions forms only in models with spectra which show a well-defined maximum, i.e. a rather rapid transition between positive and negative spectral indexes. By contrast, models with shallow maxima are less organized than the observed distribution of galaxies in space. The wavelength of the maximum defines

https://doi.org/10.1017/S0074180900110071 Published online by Cambridge University Press

the scale of the pattern: in models with different position of the maximum, λ_t, the scale of the structure changes and is always equal to the scale of the maximum. The location of high-density regions is irregular if there is no maximum within the computational box, or if the maximum is very flat.

4. Correlation function and power spectra

One possibility to express quantitatively the presence of a semiregular pattern of high- and low-density regions is to use mean diameters of voids defined by rich clusters (Einasto *et al.* 1994b). This statistics can be combined with the characteristic size of superclusters. We can also use the correlation function of rich clusters of galaxies. In the presence of a regular pattern of high- and low-density regions the correlation function has a minimum on scales $70 - 100\ h^{-1}$ Mpc due to anticorrelation between superclusters and supervoids, and a secondary maximum corresponding to cluster pairs in superclusters across supervoids. Figure 4 gives the correlation function for clusters of galaxies (Einasto *et al.* 1993), and for simulated clusters in the double power-law model and in CDM models. In CDM models the correlation function of clusters of galaxies has no secondary maximum, because the spacing of superclusters is less regular. Therefore, the correlation function confirms our previous conclusion, that the models which best represent the observations are those with a sharp transition in the initial spectra.

Experimentation with simple toy models has shown, that a secondary maximum is observed in any semiregular model, with clusters located either on grid corners, edges or surfaces. The more regular is the displacement of these structures the stronger is the secondary maximum.

Our calculations show that perturbations on large scale ($\lambda > \lambda_t$) modulate small-scale structures. If there are no large-scale perturbations, then superclusters form a very regular rectangular pattern and all superclusters have approximately equal masses. However, if the amplitude of perturbations continues to grow at scales larger than λ_t with approximately the same rate as on small scales, then the spacing of superclusters becomes irregular and the masses of superclusters differ considerably (Frisch *et al.* 1994). The best fit to the observed distribution is achieved with a Harrison-Zeldovich index $n_l = 1$ favored also by COBE observations (Smoot *et al.* 1992).

The amplitude of density fluctuations on large scales can be fixed by COBE observations. The power spectra of models are shown in Figure 4. We see that our model N2p has on large scales an amplitude within the error box permitted by COBE observations. High-density CDM model has on scales $\approx 100\ h^{-1}$ Mpc an amplitude considerably lower than the observed amplitude. Similar discrepancy was found for the correlation function on large scales by Maddox, Efstathiou and Sutherland (1990). The low-density

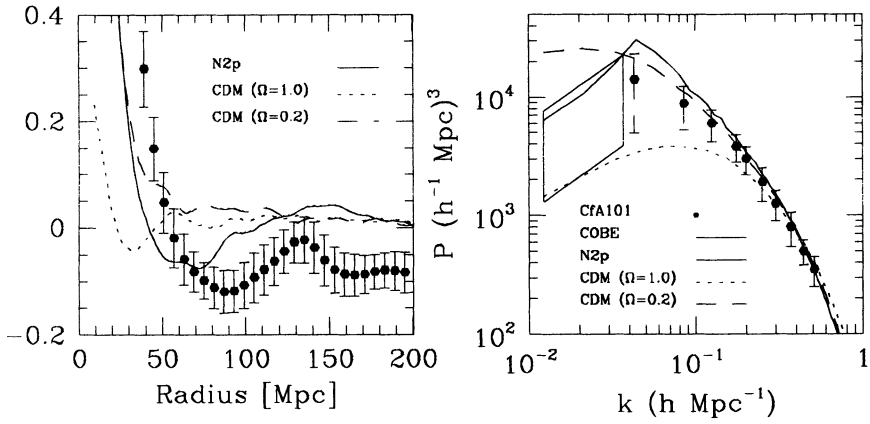

Figure 4. Left panel: The correlation function. Dots are for the observed correlation function for rich clusters of galaxies (Einasto *et al.* 1993) for the 300 h^{-1} Mpc sample in the Northern supergalactic hemisphere; the error corridor is indicated. Solid and dashed lines are for simulated clusters of the models N2p, CDM1 and CDM2. Right panel: The power spectra. Dots show the observed spectrum for galaxies (Park *et al.* 1994), the error box determined by COBE observations includes errors of both $\Omega = 1$ and $\Omega = 0.2$. Solid and dashed lines are for the spectrum of mass fluctuations of models.

CDM-model fits the spectrum of galaxies well, but on large scales it lies considerably higher than suggested by COBE data.

5. Conclusions

Difficulties with the high-density CDM model are well known (Maddox, Efstathiou and Sutherland 1990, Bahcall, Cen 1992). This is a problem of all models with a low effective spectral index, $n_s \approx -0.5$, on small scales. Also the mass distribution function of clusters of galaxies differs considerably from the observed function (Bahcall, Cen 1993, Frisch *et al.* 1994).

This problem does not arise in low-density CDM models since over the whole wavelength interval covered by ordinary galaxies ($1 - 100\ h^{-1}$ Mpc) the spectrum has a mean index $n_s \approx -1.5$ as observed. Most quantitative tests applied to this model show that it agrees well with observations (Bahcall, Cen 1992, 1993, Bahcall, Cen, Gramann 1993). However, in this case the amplitude of the spectrum continues to increase towards long wavelengths, the maximum is located at $\lambda_t \approx 500\ h^{-1}$ Mpc and is very flat. In this model the location of superclusters is much less regular than in models with a rapid transition between positive and negative spectral indexes (compare Figure 2 and Figure 3). Also this model has problems with the COBE normalization as mentioned above. To overcome the normal-

https://doi.org/10.1017/S0074180900110071 Published online by Cambridge University Press

ization problem a high bias, b, (and low value of σ_8) is adopted, but this assumption contradicts data on the fraction of matter in voids, F_v, since $b = 1/F_v \approx 1.15$ (Einasto *et al.* 1994b).

Thus we must conclude that CDM-type models, both high- and low-density, have two problems: they produce large-scale distribution of superclusters and voids which is less regular than the observed distribution, and it is difficult to reproduce simultaneously the observed power spectrum defined by galaxies and COBE data, taking into account also possible limits of the biasing factor.

ACKNOWLEDGEMENTS. Results reported here have been obtained by a collaboration between Tartu and Göttingen Observatories and European Southern Observatory. I thank my collaborators Heinz Andernach, Maret Einasto, Wolfram Freudling, Klaus Fricke, Patrick Frisch, Mirt Gramann, Ulrich Lindner, Veikko Saar, and Erik Tago for fruitful team work and permission to use our joint results before publication. This work was partly supported by the grant LDC 000 of the International Science Foundation.

References

Bahcall, N. A. 1991. *Astrophys. J.* **376**, 43.
Bahcall, N. A., Cen, R. Y. 1992. *Astrophys. J.* **398**, L81.
Bahcall, N. A., Cen, R. Y. 1993. *Astrophys. J.* **407**, L49.
Bahcall, N.A., Cen, R.Y., Gramann, M. 1993. *Astrophys. J.* **408**, L77.
Broadhurst, T.J., Ellis, R.S., Koo, D.C., Szalay, A.S. 1990. *Nature* **343**, 726.
Einasto, J., Gramann, M. 1993. *Astrophys. J.* **407**, 443.
Einasto, J., Gramann, M., Saar, E., Tago, E. 1993. *Mon. Not. R. astr. Soc.* **260**, 705.
Einasto, J., Saar, E., Einasto, M., Freudling, W., Gramann, M. 1994a. *Astrophys. J.* **429**, 465.
Einasto, M., Einasto, J., Tago, E., Dalton, G.B., Andernach, H. 1994b. *Mon. Not. R. astr. Soc.* **269**, 301.
Frisch, P., Einasto, J., Einasto, M., Freudling, W., Fricke, K.J., Gramann, M., Saar, V., Toomet, O. 1994. *Astron. Astrophys.* (in the press).
Lindner, U., Einasto, J., Einasto, M., Freudling, W., Fricke, K., Tago, E., 1994. *Astron. Astrophys.* (in the press).
Maddox, S.J., Efstathiou, G., Sutherland, W. 1990. *Mon. Not. R. astr. Soc.* **246**, 433.
Mo H.J., Deng Z.G., Xia X.Y., Schiller P., & Börner G. 1992a: *Astron. Astrophys.* **257**, 1.
Mo H.J., Xia X.Y., Deng Z.G., Börner G., & Fang, L.Z. 1992b: *Astron. Astrophys.* **256**, L23.
Park, C., Vogeley, M.S., Geller, M.J., and Huchra, J.P., 1994. *Astrophys. J.* (in the press).
Saar, V., Einasto, J., Einasto, M., Gramann, M., Tago, E., Fricke, K., Frisch, P., Lindner, U., Freudling, W., 1994. *Astrophys. J.* (submitted).
Smoot, G.F. *et al.* 1992. *Astrophys. J.* **396**, L1.
Tully, R. B., Scaramella, R., Vettolani, G., Zamorani, G. 1992. *Astrophys. J.* **388**, 9.
Vettolani, G. *et al.* 1994. In *Astronomy from Wide Field Imaging*, ed. MacGillivray, H.T., (in the press).